Stochastic Geometry Framework for THz Satellite-Airplane Network Analysis

Joonas Kokkoniemi*, Josep M. Jornet†, and Markku Juntti*
*Centre for Wireless Communications (CWC), University of Oulu, Oulu, Finland
†Department of Electrical and Computer Engineering, Northeastern University, Boston, MA, USA
Email: joonas.kokkoniemi@oulu.fi

***Abstract*—The THz frequencies (0.1–10 THz) have shown great potential for long distance satellite communications in the recent research papers. This band offers superior bandwidths compared to those enabled by the lower frequencies, with relaxed pointing requirements compared to optical systems, making the the THz band very appealing for providing backhaul connectivity on vast numbers of airplanes. At the same time, the path losses are very high and extremely directional antennas are required to operate on the links exceeding thousands of kilometers in the satellite applications. This paper derives a framework for stochastic geometry based estimation of average signal levels in THz satellite networks. Specific focus herein is on the airplane-satellite links. The produced stochastic models are shown to be exact with a simulation model. The analysis shows that while the average path losses are very high, there are antenna solutions that can overcome the losses and give respectable signal-to-noise ratios. The derived models are very useful in satellite network analysis, as well as in the link budget calculations for future high frequency satellite systems.**

I. Introduction

The future beyond 5G (B5G) and 6G wireless communications systems have been set an ambitious goal of bringing the internet to everywhere [1]. How to connect the rest of the world effectively bridging the digital divide is a major problem that requires looking outside the terrestrial networks for worldwide coverage. On the other hand, the future communication systems are set to crush the data rates of the previous generations to provide "unlimited" link speeds for the data hungry applications. For this reason, the millimeter wave band (mmWave, 30–300 GHz) and THz band (0.3–10 THz) are seen as the most promising frequency bands for the future networks for high bandwidth applications [2], [3]. When we put the two above visions together, we get an interesting and highly potential research direction: THz satellite communications.

The utilization of the THz band in satellite communications has been studied in various recent research papers [4]–[13]. Their majority focuses on channel modelling of the links in the satellite communications in different channel conditions and link types. A consensus of these mostly link specific papers is that the THz frequencies are very much suitable for satellite communications regardless of the very large path losses in these extremely long links. The main problem is to generate enough antenna gain at transmitter (Tx) and receiver (Rx). This can be achieved by, e.g., utilizing parabolic antenna structures that tend to provide very large gains at the cost of mostly mechanical beam steering. A very popular topic among current THz satellite works are related to the inter-satellite links, e.g., [10]–[13]. The utilization of the THz frequencies therein interesting because of lack of the atmospheric losses. Based on the works listed above, the THz satellite networks are feasible in principle, but there is still a lot of work and analysis ahead to properly understand the limitations and boundaries of the THz satellite links and networks. This is especially the case with the ground-satellite, ground-airplane, and airplane-satellite links that experience very high frequency selective atmospheric losses.

Stochastic geometry is a very powerful tool for various wireless network problems. It can be used to study the average network behavior with mathematical tools [14]–[20]. We have used the stochastic geometry in the past on interference modelling in different network setups [17]–[20]. Rather than modelling the interference, the goal of this paper is to model the average received signal strength and the path loss at an airplane from a network of satellites utilizing stochastic geometry. The work herein focuses specifically on the THz band satellite networks following our previous channel modeling work given in [4]. Therefore, the propagation features in the atmosphere are very important in the derived models, although, the resultant stochastic models can be utilized in pure space applications as well. By assuming that the airplane antenna sees everything above its horizon, the field of view of the airplane forms mathematically simple spherical cap. Then we can rather straightforwardly utilize the stochastic geometry to model the aggregated signals at the airplane. As such, this paper focuses on the downlink modelling of the airplane-satellite networks.

There are few papers specifically on modelling the satellite networks with stochastic geometry [21]–[23]. However, none of them specifically considers THz band communications, and thus, the propagation models are fundamentally different. A similar spherical cap approach as herein has been used in the past to model the satellite locations in space in [21], [22]. The details of the spherical cap modelling is given in the next section. Specifically in [21], the authors model the nearest satellite locations as well as the interfering satellites with the spherical cap. In [22], the authors use the spherical cap model to derive the probability of service at certain minimum elevation angle, and then some related modelling of the distance distributions and the outage probabilities.

In this paper, we model the mean signal level obtained from

a network of random satellites using stochastic geometry and by utilizing the spherical cap as a airplane field of view. To the best of our knowledge, this is the first paper to consider the stochastic geometry in THz satellite networks to model the average received signal levels.

The rest of this paper has been organized as follows. The system model, system geometry, and the link model are given in Sec. II, the mean signal level via stochastic geometry is derived in Sec. III, the numerical results and validations are given in Sec. IV, and some conclusions and discussion are given in Sec. V.

II. System and Link Models

In this section, we go through the system model and its geometry. Based on the system geometry, we can define the link models used later in the stochastic modelling of the signal response in satellite network.

A. System Model and Geometry

The system model utilized in this work is shown in Fig. 1. The primary goal herein is to model the received signal strength from a network of satellites using stochastic geometry. In other words, we utilize the propagation geometry via mathematical tools to estimate the aggregated response of the system. The aggregated signal at the airplane is assumed to come from a random constellation of satellites. In this setting, the antenna at the airplane is assumed to see the elevation angles from ± 90 degrees from the zenith and 360 degrees in the azimuth. Then, the field of view of the airplane with the airplane and satellite altitudes form a spherical cap. Any satellite within the area of the spherical cap is thereby visible to the airplane. The model results in a geometry described by simple mathematical expressions.

The geometry of the spherical cap model in satellite-airplane use case is given below. The minimum distance between the airplane and the satellite is given by the direct zenith distance as (see Fig. 1)

$$r_{min} = h_s - h_a, \tag{1}$$

where h_a is the altitude of the airplane, h_s is the altitude of the satellite. The maximum distance is taken along the horizon of the airplane to the satellite's orbit as

$$r_{max} = (R + h_s)\sin(\theta), \tag{2}$$

where R is the radius of Earth and θ is the angle between the airplane and satellite looked from the center of the Earth, which is further given by

$$\theta = \cos^{-1}\left(\frac{R + h_a}{R + h_s}\right). \tag{3}$$

As mentioned above, we assume that the airplane is served by satellites spread on a surface of a spherical cap determined by the satellite and airplane altitudes, and the airplane horizon. Then the total area of the spherical cap where the satellites reside is given by

$$A_{\text{sp}} = 2\pi(R + h_s)^2(1 - \cos(\theta)). \tag{4}$$

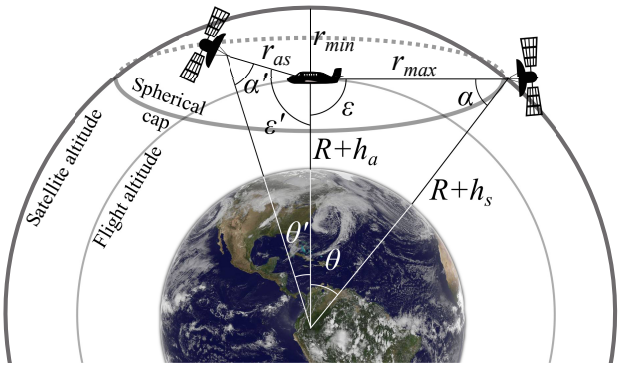

Fig. 1. System model and geometry utilized in this paper. Picture of Earth by NASA/NOAA's GOES Project [24].

Furthermore, we defined the geometry of the generic satellite system in [4]. From there, we get the distance from the airplane to satellite as

$$r_{as}(\theta) = \sqrt{(R + h_a)^2 + (R + h_s)^2 - 2(R + h_a)(R + h_s)\cos(\theta)}, \tag{5}$$

and the distance (or path) through the atmosphere is

$$r_{\text{atm}}(\theta, x) = (R + h_a)\cos(\epsilon) + \frac{1}{2}\sqrt{(-2(R + h_a)\cos(\epsilon))^2 - 4((R + h_a)^2 - (R + x)^2)}, \tag{6}$$

where x is the vertical distance/path through the atmosphere, and ϵ is the angle between Earth's core and satellite looked from the airplane;

$$\epsilon = 180^\circ - \alpha - \theta, \tag{7}$$

where α is the angle between the satellite and the airplane looked from the satellite;

$$\alpha = \sin^{-1}\left(\frac{(R + h_a)\sin(\theta)}{r_{as}(\theta)}\right). \tag{8}$$

This completes the geometry of the system. Next we look into the link model before going to utilize the above geometry in estimating the average received power via stochastic geometry.

B. Link Model

The total received signal power was derived in [4] and is given as

$$S(f, r_{as}(\theta)) = \frac{c^2 P_{\text{Tx}} G_{\text{Tx}} G_{\text{Rx}}}{(4\pi r_{as}(\theta) f)^2} e^{-\int_{h_a}^{h_l} \kappa_a(f, r_{\text{atm}}(\theta, x))dx}, \tag{9}$$

where P_{Tx} is the transmit power, G_{Tx} and G_{Rx} are the Tx and Rx antenna gains, respectively, f is the frequency, c is the speed of light, h_l is the vertical limit of the atmosphere, and $\kappa_a(f, r)$ is the absorption coefficient. Detailed calculation of the absorption coefficient can be found in our previous work in [4]. Here we assume that the upper bound of the atmosphere is at 500 km height from the ground, and hence, $h_l = 500$ km. Notice that we do not take into account possible cloud losses, or any other losses, such as antenna misalignment [25]

herein, but we just focus on the ideal line-of-sight (LOS) case. However, the other losses would be included in the above signal model as in [4]. We keep the expressions as simple as possible due to focus on derivation of the fundamental model for stochastic average received power in THz satellite networks to gain the core insights to the problem.

Satellite communications means extremely long link distance and the THz frequencies experience very high path loss as a function of distance. Hence, these satellite links require in practice large fixed aperture antennas. The parabolic reflector antennas give extremely high antenna gains as a function of the antenna diameter, but even better, their gain increases as a function of frequency for fixed size aperture. The gain of such ideal parabolic reflector antenna is given as

$$G(f) = A_e \left(\frac{\pi d_A}{\lambda} \right)^2, \tag{10}$$

where A_e is the aperture efficiency, d_A is the diameter of the reflector, and λ is the wavelength. It is important to recognize a limitation of these types of antennas. We derive a model for aggregated signal power at airplane. However, the parabolic reflector antennas with extremely high gain can only see a single satellite unless the satellites are very close to each other. Therefore, in the numerical results we focus on the average signal power from a single satellite even if the theories do not limit the number of satellites. The antenna model assumption herein does limit the practical number of satellites as we cannot beamform into multiple directions at the same time.

III. Stochastic Modeling of Airplane-Satellite Signals

In this section, we derive the stochastic model for the average received signal power.

A. Preliminaries

As mentioned above, we utilize the stochastic geometry for modelling the aggregated desired signal rather than the interference. The derivation of the models, including the generic assumptions, are similar to our previous works and especially the ones in [17]. The core assumptions are as follows. We assume that the satellites send in an uncoordinated fashion and independently to each other. The satellites are evenly and randomly distributed about the spherical cap. The number of serving satellites follows a Poisson distribution. Hence, the received signals follow Poisson point process (PPP). In the next section, we give the derivation of the average receiver signal power as well as the average path loss.

B. Average Received Power

The total aggregated signal power can be given as

$$S_{\text{tot}}(f) = \sum_{i \in \Phi} S(f, r_{as}^i(\theta)), \tag{11}$$

where Φ is the set of serving satellites. We can solve the average receive signal power from the Laplace transform of the aggregated signal power. That is given by

$$\mathcal{L}_{S_{\text{tot}}}(s) = \mathbb{E}\left[\exp\left(-s \sum_{i \in \Phi} S(f, r_{as}^i(\theta)) \right) \right]. \tag{12}$$

This is the probability generating functional (PGFL) of the random process. Assuming that the satellite transmissions are Poisson distributed, the above equation can be further given as [14]

$$\mathcal{L}_{S_{\text{tot}}}(s) = \exp\left(-\int_{\Theta} \Big[1 - \exp(S(f, r_{as}(\Theta))s) \Big] \Lambda(\Theta) d\Theta \right), \tag{13}$$

where Θ is the solid angle for integration over the space and $\Lambda(\Theta)$ is the intensity function of the PPP. This intensity function in the case of spherical cap can be derived as

$$\Lambda(\Theta) = p\lambda_s 2\pi (R + h_s)^2 \sin(\theta), \tag{14}$$

where λ_s is the density of the satellites over the area of the spherical cap, which is given by

$$\lambda_s = \frac{N}{2\pi (R + h_s)^2 (1 - \cos(\theta))}, \tag{15}$$

where N is the average number of visible satellites, i.e., the density is given by the number of potentially serving satellites over the horizon of the airplane. Furthermore, p is the probability that a visible satellite serves the airplane (p =1 assumed here), and the area term is given by $2\pi(R+h_s)^2 \sin(\Theta)$. This is derived from the expression for the area of the spherical cap,

$$A_{\text{sp}} = \int_0^{2\pi} \int_0^{\theta} r^2 \sin(\beta) d\beta d\phi, \tag{16}$$

with a circularly symmetric azimuth plane, where ϕ is the azimuth angle and θ is the elevation angle. Circularly symmetric azimuth plane, as we have here (see Fig. 1), yields the area of the spherical cap given in (4) with $r = (R + h_s)$.

From above, we can give the Laplace transform as

$$\mathcal{L}_{S_{\text{tot}}}(s) = \exp\Bigg(-2\pi\lambda_s (R + h_s)^2 \times \int_0^{\theta} \Big[1 - \exp(S(f, r_{as}(\phi))s) \Big] \sin(\phi) d\phi \Bigg). \tag{17}$$

The nth moment of the interference power can be calculated as [16]

$$\mathbb{E}[S_{\text{tot}}^n] = (-1)^n \frac{d^n}{ds^n} \mathcal{L}_{S_{\text{tot}}}(s) \Big|_{s=0}. \tag{18}$$

The average aggregated signal power at the airplane can hence be derived from the first moment of the above Laplace

transform as

$$S_{\text{ave}}(f) = \frac{c^2 N P_{\text{Tx}} G_{\text{Tx}} G_{\text{Rx}}}{(1-\cos(\theta))(4\pi f)^2} \times \int_0^{\theta} \frac{\sin(\phi)}{r_{\text{as}}^2(\phi)} \exp\left(- \int_{h_a}^{h_l} \kappa_a(f, r_{\text{atm}}(\phi, x)) dx \right) d\phi. \quad (19)$$

This is the last piece of the puzzle and completes the derivation. Unfortunately we cannot solve this equation in a closed form due to the database based absorption coefficient. Furthermore, the line shape function is piece-wise defined about the atmospheric pressure due to mixture of pressure broadening and Doppler broadening when propagating through the atmosphere [4]. Also, atmospheric temperature and pressure are piece-wise defined about the altitude in the US Standard Atmospheric model [26], which we use partially in the derivation of the satellite channels in [4]. As a consequence, expression (19) can only be evaluated numerically. However, this does not necessarily decrease the accuracy of the model. It will be shown in the numerical results to give the exact response based on a comparison to a simulation model.

From (19) we see that this expression can also be utilized in estimating the average path loss. The average path loss of a single link is given by

$$\text{PL}_{\text{ave}}(f) = \frac{(1-\cos(\theta))(4\pi f)^2}{c^2} \times \left(\int_0^{\theta} \frac{\sin(\phi)}{r_{\text{as}}^2(\phi)} \exp\left(- \int_{h_a}^{h_l} \kappa_a(f, r_{\text{atm}}(\phi, x)) dx \right) d\phi \right)^{-1}. \quad (20)$$

This is shown to be exact in the numerical results.

IV. Numerical Results

In this section, we report the numerical results based on the derived models against simulations to verify the derivations. The assumptions herein are as follows. The transmit power of a satellite is 1 Watt, the airplane has 0.5 meter diameter antenna and the satellite has 1 meter diameter antenna with aperture efficiency of 70% at both ends (gains shown in Fig. 2), and the airplane altitude is 11 km. As mentioned above, due to the parabolic reflector antenna assumption, we assume that the airplane is served by one satellite on the average, as we cannot practically beamform towards many satellites at the same time. Thereby, the results herein represent the average channel gains and the received powers from a single satellite, even if the theories would allow multiple serving satellites. The simulation model was made by randomly dropping a single satellite on a spherical cap and calculating the received signal with (9) based on the position of the satellite and the airplane. The simulation results were obtained as an average over 10,000 channel realizations.

Firstly, Fig. 2 gives the theoretical mean path loss and the simulated one for a satellite at 400 km height from the ground. The total antenna gain (Tx+Rx) has been given in the figure

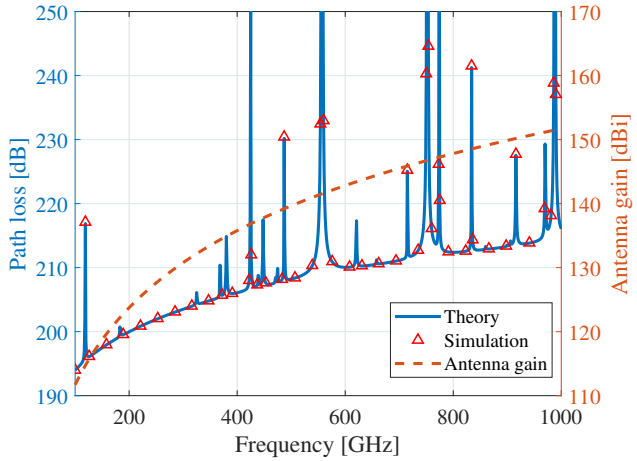

Fig. 2. The mean path loss as a function of frequency for the theoretical and simulation models at 11 km airplane and 400 km satellite altitudes. The combined antenna gain is given by red dashed line on the right-hand scale.

as well with the red dashed line. The left-hand axis gives the path loss and the right-hand axis gives the combined antenna gain as a function of frequency. The path loss itself was more accurately analyzed in [4] and it can be summarized as being very large, requiring parabolic antenna type solutions to give sufficient antenna gain for the THz band operation. The more important takeaway here is that the theoretical mean path loss given by (20) is an exact match with the simulated path loss. As the mean path loss was derived directly from the main result, the mean received signal power, this confirms that the theoretical models are correct.

Fig. 3 gives the average theoretical received signal power according to (19) for a satellite altitude of 400 km. The simulated values have been given as well. Furthermore, we included the noise floors for various signal bandwidths as a reference assuming relatively pessimistic 10 dB noise figure at the receiver. Also, the maximum and minimum signal powers have been plotted. The minimum signal power is obtained when the satellite is directly at the horizon of the airplane and maximum signal power is obtained when the satellite is directly at the zenith of the plane.

We can see few interesting features from Fig. 3. Firstly, the maximum and minimum signal powers show the large difference in the molecular absorption. The horizontal path experiences significantly higher absorption loss as the path through the atmosphere is much longer. The overall path loss is also remarkably higher, but this is mainly explained by the longer path length from the satellite to the airplane (see Table I). The average received signal tends to lean slightly towards the minimum signal level due to the spherical geometry. That is, spatially evenly distributed satellites emphasize the higher θ angles because of the size of an area element on a surface of a (unit) sphere is $\sin(\beta)d\beta d\phi$ (see (16)). Therefore, the sphere point picking principle was applied in the simulation model to distribute the satellites evenly in the spatial domain.

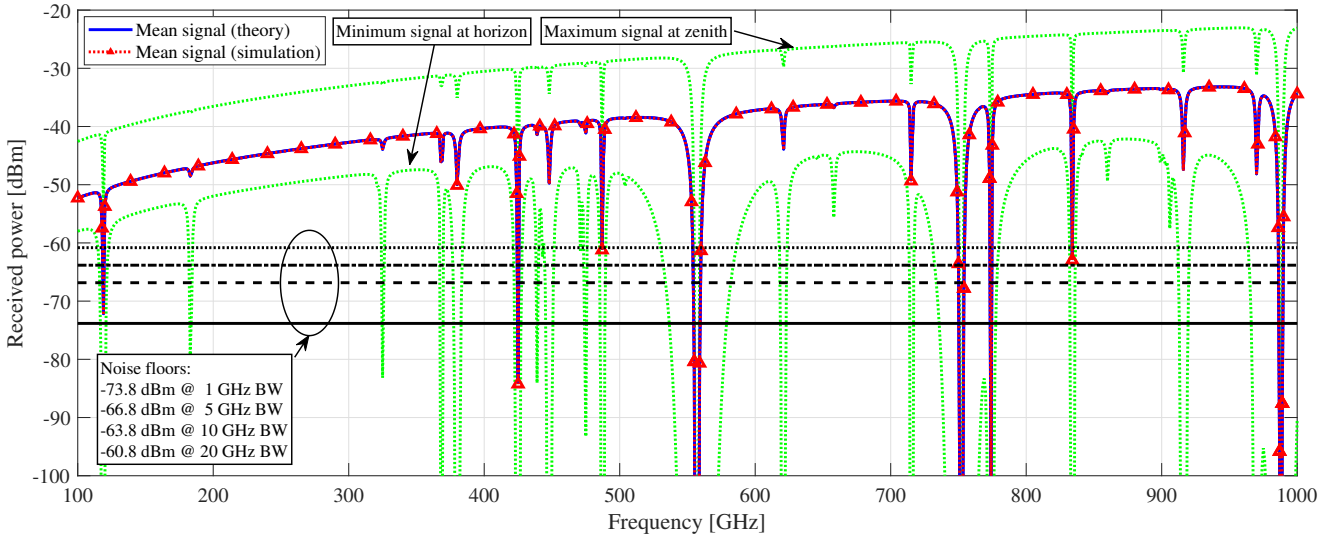

Fig. 3. The average signal levels by the theoretical and simulation model, as well as the maximum and minimum signal levels with the illustration of some noise floor levels for various bandwidths (BW in this figure). The airplane altitude is 11 km and the satellite altitude is 400 km.

TABLE I
SATELLITE TO AIRPLANE LINK'S MINIMUM AND MAXIMUM DISTANCES AT 11 KM AIRPLANE ALTITUDE, AND THE ANGLE θ (SEE FIG. 1)

Satellite altitude	r_{min}	r_{max}	θ
400 km	389 km	2263 km	19.5°
800 km	789 km	3272 km	27.1°
2000 km	1989 km	5920 km	40.3°
5000 km	4989 km	9415 km	55.8°
36000 km	35989 km	41894 km	81.3°

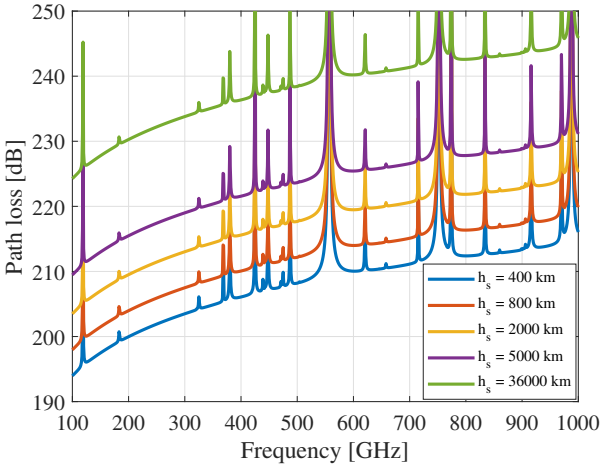

Fig. 4. The mean path losses for various satellite altitudes.

We can further see that while there is clearly room between the noise floors and the received signal powers, we only accounted for the ideal LOS link. The real path loss could be even significantly higher depending on the atmospheric conditions and the altitude of the airplane. We can see in Fig. 4 that the mean path loss increases quite sharply with the altitude of the satellite with the corresponding link geometries given in Table I. Hence, larger antennas may be required depending on the exact system geometry.

V. CONCLUSIONS AND DISCUSSION

We presented a framework for stochastic modelling of average signal levels in THz satellite networks. The derived models were shown to be exact by simulations. The models presented here can be utilized to estimate the average behavior network, and the corresponding service outage probabilities. The path losses in the THz band are very large on extremely long links, but those can be compensated with large fixed aperture antennas. The channel loss is especially high on satellite links penetrating the atmosphere. Whereas the models herein were derived for the airplane-satellite links, the similar spherical cap approach could be taken for a ground stations as well, or even on inter-satellite networks with varying satellite altitudes. Although, the path loss increases significantly for the ground links due to thick atmosphere close to ground that limits the usable frequencies below 300 GHz [4].

The THz band has a great potential for satellite applications. Very large spectral resources ensure a lot of room for various applications to co-exist. On the other hand, the spectral resources can be divided among large numbers of airplanes to provide frequency diversity. One great challenge is the very high antenna directivity and, consequently, how to achieve this gain in a dynamically beamforming structure. However, the relative motion of bodies in extremely large distance links is not high, making it easier to accomplish, e.g., by mechanical

beamforming [27]. Besides those, regulatory issues and co-existence with passive Earth exploration services limit the usability the full THz band in space applications [5], [28]. Regardless of the mountain of research problems, the THz satellite communications is on the radar for many potential applications in the future networks, such as the airplane to satellite communications and remote area communications.

ACKNOWLEDGEMENT

This work was supported by the Horizon 2020, European Union's Framework Programme for Research and Innovation, under grant agreement no. 871464 (ARIADNE). It was also supported in part by the Academy of Finland 6Genesis Flagship under grant no. 318927. This work was also supported in part by the US Air Force Research Laboratory Grant FA8750-20-1-0200 and the US National Science Foundation Grants CNS-2011411.

REFERENCES

[1] H. Saarnisaari, S. Dixit, M.-S. Alouini, A. Chaoub, M. Giordani, A. Kliks, M. Matinmikko-Blue, and N. Zhang, Eds., *6G White Paper on Connectivity For Remote Areas*, ser. 6G Research Visions. 6G Flagship, University of Oulu, 2020, no. 5. [Online]. Available: http://urn.fi/urn:isbn:9789526226750

[2] I. F. Akyildiz, J. M. Jornet, and C. Han, "Terahertz band: Next frontier for wireless communications," *Elsevier Phys. Commun.*, vol. 12, pp. 16–32, Sep. 2014.

[3] M. Latva-Aho and K. Leppänen, Eds., *Key drivers and research challenges for 6G ubiquitous wireless intelligence*, ser. 6G research visions. University of Oulu, Sep. 2019, no. 1.

[4] J. Kokkoniemi, J. M. Jornet, V. Petrov, Y. Koucheryavy, and M. Juntti, "Channel modeling and performance analysis of airplane-satellite terahertz band communications," *IEEE Transactions on Vehicular Technology*, vol. 70, no. 3, pp. 2047–2061, 2021.

[5] A. J. Alqaraghuli, H. Abdellatif, and J. M. Jornet, "Performance analysis of a dual terahertz/ka band communication system for satellite mega-constellations," in *2021 IEEE 22nd International Symposium on a World of Wireless, Mobile and Multimedia Networks (WoWMoM)*, 2021, pp. 316–322.

[6] J. Y. Suen, M. T. Fang, S. P. Denny, and P. M. Lubin, "Modeling of terabit geostationary terahertz satellite links from globally dry locations," *IEEE Transactions on Terahertz Science and Technology*, vol. 5, no. 2, pp. 299–313, 2015.

[7] M. Saqlain, M. N. Idrees, S. Wang, and X. Yu, "Channel modeling and performance analysis of fixed terahertz Earth-satellite links in the low- and mid-latitude regions," *Optical Engineering*, vol. 60, no. 3, pp. 1 – 16, 2021. [Online]. Available: https://doi.org/10.1117/1.OE.60.3.036103

[8] M. Civas and O. B. Akan, "Terahertz wireless communications in space," *arXiv*, pp. 1–7, 2021. [Online]. Available: https://arxiv.org/abs/2110.00781

[9] M. Saqlain, N. M. Idrees, X. Cao, X. Gao, and X. Yu, "Feasibility analysis of opto-electronic thz earth-satellite links in the low- and mid-latitude regions," *Appl. Opt.*, vol. 58, no. 25, pp. 6762–6769, Sep 2019. [Online]. Available: http://www.osapublishing.org/ao/abstract.cfm?URI=ao-58-25-6762

[10] S. Nie and I. F. Akyildiz, "Channel modeling and analysis of inter-small-satellite links in terahertz band space networks," *IEEE Transactions on Communications*, pp. 1–1, 2021.

[11] L. Bai, Z. Zhu, and X. Li, "Analysis of THz space communication link based on STK," *IOPscience Journal of Physics: Conference Series*, vol. 1971, no. 1, p. 012073, jul 2021. [Online]. Available: https://doi.org/10.1088/1742-6596/1971/1/012073

[12] S. U. Hwu, K. B. deSilva, and C. T. Jih, "Terahertz (thz) wireless systems for space applications," in *IEEE Sens. Appl. Symp. Proc.*, 2013.

[13] J. Yang, H. Li, and Z. Xu, "Analysis of channel characteristics between satellite and space station in terahertz band based on ray tracing," *Radio Science*, vol. 56, no. 9, p. e2021RS007290, 2021, e2021RS007290 2021RS007290. [Online]. Available: https://agupubs.onlinelibrary.wiley.com/doi/abs/10.1029/2021RS007290

[14] M. Haenggi and R. K. Ganti, "Interference in large wireless networks," *Foundations and Trends in Networking*, vol. 3, no. 2, pp. 127–248, Nov. 2008.

[15] M. Haenggi, J. G. Andrews, F. Baccelli, O. Dousse, and M. Franceschetti, "Stochastic geometry and random graphs for the analysis and design of wireless networks," *IEEE J. Sel. Areas Commun.*, vol. 27, no. 7, pp. 1029–1046, Sep. 2009.

[16] H. ElSawy, E. Hossain, and M. Haenggi, "Stochastic geometry for modeling, analysis, and design of multi-tier and cognitive cellular wireless networks: A survey," *IEEE Commun. Surveys Tuts.*, vol. 15, no. 3, pp. 996–1019, Jun. 2013.

[17] J. Kokkoniemi, J. Lehtomäki, and M. Juntti, "Stochastic geometry analysis for mean interference power and outage probability in thz networks," *IEEE Trans. Wireless Commun.*, vol. 16, no. 5, pp. 3017–3028, May 2017.

[18] J. Kokkoniemi, A. Boulogeorgos, M. Aminu, J. Lehtomäki, A. Alexiou, and M. Juntti, "Stochastic analysis of indoor THz uplink with co-channel interference and phase noise," in *Proc. ICC Workshops [accepted]*, June 2020, pp. 1–6.

[19] J. Kokkoniemi, J. Lehtomäki, and M. Juntti, "Stochastic analysis of multi-tier nanonetworks in thz band," in *Proc. ACM Int. Conf. Nanoscale Comput. Commun.*, 2017, pp. 1–6.

[20] ——, "Stochastic geometry analysis for band-limited terahertz band communications," in *IEEE Vehic. Techol. Conf. (spring)*, 2018, pp. 1–5.

[21] N. Okati, T. Riihonen, D. Korpi, I. Angervuori, and R. Wichman, "Downlink coverage and rate analysis of low earth orbit satellite constellations using stochastic geometry," *IEEE Transactions on Communications*, vol. 68, no. 8, pp. 5120–5134, 2020.

[22] D.-H. Jung, J.-G. Ryu, W.-J. Byun, and J. Choi, "Performance analysis of satellite communicationsystem under the shadowed-rician fading: A stochastic geometry approach," *arXiv*, pp. 1–12, Apr. 2021. [Online]. Available: https://arxiv.org/abs/2104.13010

[23] A. Talgat, M. A. Kishk, and M.-S. Alouini, "Stochastic geometry-based analysis of leo satellite communication systems," *IEEE Communications Letters*, vol. 25, no. 8, pp. 2458–2462, 2021.

[24] "Nasa/noaa's goes project," March 2014. [Online]. Available: https://www.nasa.gov/content/three-atmospheric-dragons-low-pressure-areas-around-the-us/

[25] J. Kokkoniemi, A.-A. A. Boulogeorgos, M. Aminu, J. Lehtomäki, A. Alexiou, and M. Juntti, "Impact of beam misalignment on THz wireless systems," *Elsevier Nano Communication Networks*, vol. 24, pp. 1–9, May 2020.

[26] "U.S. standard atmosphere 1976," NASA, Tech. Rep., 1976.

[27] A. J. Alqaraghuli, A. Singh, and J. M. Jornet, "Novel CubeSat combined antenna deployment and beam steering method using motorized rods for terahertz space networks," in *IEEE Conference on Antenna Measurements and Applications*, Nov. 2021.

[28] S. Priebe, D. M. Britz, M. Jacob, S. Sarkozy, K. M. K. H. Leong, J. E. Logan, B. S. Gorospe, and T. Kurner, "Interference investigations of active communications and passive earth exploration services in the thz frequency range," *IEEE Transactions on Terahertz Science and Technology*, vol. 2, no. 5, pp. 525–537, 2012.